

periodically spaced crystallographic shear (CS) planes. The CS planes delimit quasi two-dimensional blocks of the perovskite structure with a thickness of $(n-2)$ BO_6 octahedra, n being the number of the homologue in the series.

Using the appropriate chemical composition and thermal treatment conditions we have isolated in a single phase form different members of the homologous series with $n = 4$ ($\text{Pb}_{4-2x}\text{A}_{2x}\text{Fe}_4\text{O}_{10}$ ($\text{A} = \text{Sr}, \text{Ba}$)), $n = 5$ ($\text{Pb}_{2.9}\text{Ba}_{2.1}\text{Fe}_4\text{TiO}_{13}$, $\text{Pb}_2\text{Ba}_2\text{BiFe}_5\text{O}_{13}$), $n = 6$ ($\text{Pb}_{3.8}\text{Bi}_{0.2}\text{Ba}_2\text{Fe}_{4.2}\text{Ti}_{1.8}\text{O}_{16}$, $\text{PbBaBiFe}_3\text{O}_8$) and $n = 7$ ($\text{Pb}_{4.5}\text{Bi}_{0.2}\text{Ba}_{2.4}\text{Fe}_{4.9}\text{Ti}_{2.1}\text{O}_{19}$) [1], [2].

The crystal structures of the obtained compounds have been determined using a combination of diffraction and electron microscopy techniques: X-ray (XRD) and neutron powder diffraction (NPD), electron diffraction (ED), and high angle annular dark field scanning transmission electron microscopy (HAADF-STEM). The compounds crystallize in an orthorhombic crystal system with the lattice parameters $a \approx a_p\sqrt{2}$, $b \approx b_p$, $c \approx 9.7\text{\AA} + (n-2)a_p\sqrt{2}$, where $a_p \approx 4.06\text{\AA}$. The space groups are $Pnma$, $Ammm$ and $Imma$ for the 4th, 5th and 6th members, respectively. The $\text{A}_n\text{B}_n\text{O}_{3n-2}$ structures can be represented as a sequence of atomic layers $-\text{ABO}-(\text{O}_2-\text{ABO})_{n-2}-\text{O}_2-\text{ABO}-\text{ABO}-(\text{O}_2-\text{ABO})_{n-2}-\text{O}_2-\text{ABO}-$. HAADF-STEM reveals a long range ordered sequence of the perovskite modules with a uniform thickness for members with $n = 4-6$.

In this type of structures, the cations are partially ordered. At the CS planes, tunnels are created in which only the lead and bismuth cations are situated. The formation of tunnels allows the spatial accommodation of the lone electron pair of these cations. The coordination number of the B cations at the CS planes is 5 and these BO_5 tetragonal pyramids are occupied exclusively by Fe^{3+} cations. The remaining Fe^{3+} cations as well as Ti^{4+} cations are located in the BO_6 octahedra of the perovskite modules. The CS planes introduce edge sharing connections of the transition metal-oxygen polyhedra at the interface between the perovskite blocks. This results in intrinsically frustrated magnetic couplings between the perovskite blocks due to a competition of the exchange interactions between the edge- and the corner-sharing metal-oxygen polyhedra.

[1] I. Nikolaev, H. D'Hondt, A. Abakumov, A. Balagurov, I. Bobrikov, D. Sheptyakov, V. Pomjakushin, K. Pokholok, D. Filimonov, G. Van Tendeloo, E. Antipov, *Phys. Rev. B* **2008**, *78*, 024426. [2] A. Abakumov, J. Hadermann, M. Batuk, H. D'Hondt, O. Tyablikov, M. Rozova, K. Pokholok, D. Filimonov, D. Sheptyakov, A. Tsirlin, D. Niermann, J. Hemberger, G. Van Tendeloo, E. Antipov, *Inorganic Chemistry* **2010**, *49* (20), 9508-9516.

Keywords: perovskite, homologous series, lead

MS79.P03

Acta Cryst. (2011) **A67**, C693

Electron crystallography based on inverse dynamic scattering

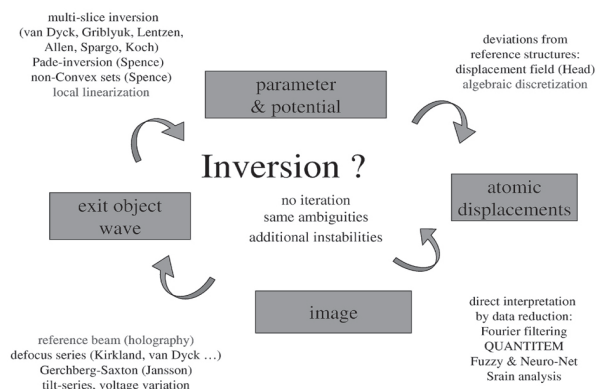
Kurt Scheerschmidt, *Max Planck Institut für Mikrostrukturphysik, Weinberg 2, Halle-Saale (Germany)*. E-mail: schee@mpi-halle.de

Electron crystallography and electron microscope tomography may enhance structure investigations via local object analysis. However, this has in contrast to X-ray techniques the disadvantage, that an ill-posed inverse problem for the highly nonlinear dynamical theory has to be solved. Fig. 1 schematically shows all necessary steps of the object analysis: anticlockwise the trial-and-error technique, clockwise the direct solution of the inverse problem. Authors which proposed partial solutions are listed, too. Details are to be found in [1] with respective references. In [1], [2] also a special solution of the inverse problem for the local parameter analysis is given. Step 1 of the inversion is solved, by replacing the image by a hologram or a defocus series, which makes the problem linear, and finding the exit object wave by inverse Fourier transform. Step 2 yielding the object structure directly from the exit

wave, is the real challenge of inversion. Step 3, the analysis of lattice defects, has no explicit solution yet.

The solution proposed here for step 2 can be characterized in short as follows [1], [2]: The first step of inversion yields the moduli and phases for all reflections of the experimental exit plane waves Φ^{exp} as function of lateral (pixel) positions (i,j) . Theoretical waves Φ^{th} are then calculated using the dynamical scattering matrix \mathbf{M} for an a priori model characterized by the number of beams and the scattering potential \mathbf{V} . With a suitable experimentally predetermined a priori beam orientation \mathbf{K}_0 and sample thickness t_0 as a free parameter, a perturbation approximation yields both Φ^{th} and \mathbf{M} as linear functions of the parameter to be retrieved. Its analytic form enables the inverse solution of $\|\Phi^{\text{exp}} - \Phi^{\text{th}}\| = \text{Min}$ yielding directly for each image pixel the local thickness $t(i,j)$, the local beam orientation $\mathbf{K}(i,j)$, and further data of the parameter space.

The linearization transforms the ill-posed problem to a well posed one and enables the analytic inverse. However, the solution is ill-conditioned. With the generalized and regularized inverse in [2] an enhancement of the solution is given. By applying second order perturbation and using a mixed type potential $V(i,j) = q_k(i,j) V^k$ in [1] with the parameters $q_k(i,j)$ also local potential variations can be retrieved [3]. Smoothing, coupling of different parameters via additional a priori information, including the iteration of the start values, if the retrieved parameter goes beyond the confidence region, finally help to avoid modeling errors.



[1] K. Scheerschmidt, *Ultramicroscopy* **2010**, *110*, 543-547. [2] K. Scheerschmidt *Journal of Microsc.* **1998**, *190*, 238-248. [3] K. Scheerschmidt *Proc. 17. Int. Microsc. Congr. Brazil* **2010**, *18.4*.

Keywords: inverse problems, electron holography, analytic approximation

MS79.P04

Acta Cryst. (2011) **A67**, C693-C694

Automatic diffraction tomography (ADT) with precession on 6H-SiC and NiTe

Enrico Mugnaioli,^a Eleni Sarakinou,^b Christos Lioutas,^b Nikolaos Vouroutzis,^b Nikolaos Frangis,^b Ute Kolb,^a Stavros Nicolopoulos,^c *^aInstitut für Physical Chemistry, Johannes Gutenberg -University, Welderweg 11, 55099 Mainz (Germany).* *^bDepartment of Physics, Aristotle University of Thessaloniki, 54124 Thessaloniki, (Greece).* *^cNanoMEGAS SPRL, Blvd Edmond Machtens 79, B-1080 Brussels, (Belgium).* E-mail: mugnaioli@uni-mainz.de

Automated electron Diffraction Tomography (ADT) in combination with precession electron diffraction (PED) has been recently used in the investigation of nano-crystalline materials. By the use of this method

it is possible to sample and reconstruct the 3D diffraction space, to automatically determinate the unit cell parameters and to integrate electron diffraction intensity data sets able to deliver the crystal structure by direct methods. [1], [2]. 3D data are acquired through a sequential tilt of the selected nano-crystal around an arbitrary axis. The tilt step is usually 1° and tilt range of ± 60° can be reached. An example of 3D reconstructed diffraction space is shown in Figure 1. Such a data set contains nearly all the reflections present in the covered wedge of the reciprocal space. Combining electron beam precession (NanoMEGAS) with tomographic diffraction data acquisition principle allows proper integration of reflection intensities and drastically reduces dynamical effects. In the last three years more than 25 crystal structures (organic and inorganic) have been solved ab-initio with ADT. ADT is especially effective for data collection from beam sensitive materials because it uses low illumination conditions in STEM mode and includes devoted routines for electron dose distribution. Here we report for the first time ADT study on reference 6H-SiC semiconductor and NiTe binary compound samples. Those materials have physical properties which are suitable for applications into electronic systems as the wide energy gap of the 6H-SiC is suitable for UV-detectors and blue light lasers. Using ADT/PED we were able to reconstruct accurately their diffraction space, find their cell parameters and solve ab-initio their structure with a kinematical approximation (I proportional to F_{hkl}^2). All the atoms (C, Si and Ni, Te) were localized and the solution show a residual R of 13%, remarkably low for electron diffraction data.

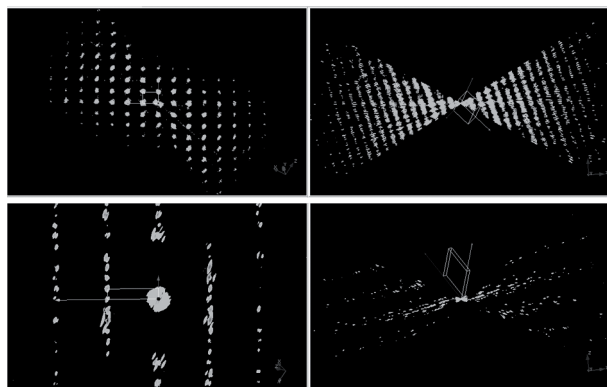


Figure 1: ADT reconstructed 3D diffraction space and unit cell for NiTe and SiC. Upper: NiTe along (001) (left) and tilt axis (right). Bottom: SiC along (001) (left) and tilt axis (right).

[1] U. Kolb, T. Gorelik, M. T. Otten, *Ultramicroscopy* **2008**, 108, 763-772. [2] E. Mugnaioli, T. Gorelik, U. Kolb, *Ultramicroscopy* **2009**, 109, 758-765

Keywords: electron diffraction, precession, structure solution

MS79.P05

Acta Cryst. (2011) A67, C694

Huge unit cell $\text{Sr}_{64.1}\text{Bi}_{27.7}\text{Ni}_{8.2}\text{O}_x$ solved by precession electron diffraction

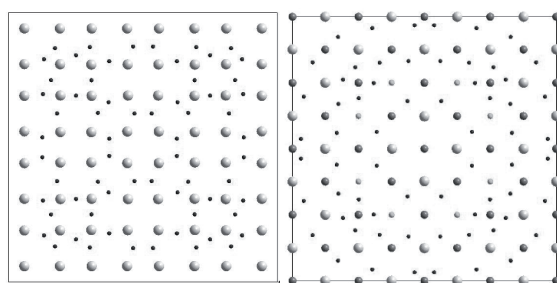
Holger Klein,^a M. Bacia,^a A. Rageau,^a P. Strobel,^a M. Gemmi,^b
^aInstitut Néel, Grenoble, France ^bDipartimento di Scienze della Terra 'Ardito Desio', Sezione di Mineralogia, Milano, (Italy). E-mail: holger.klein@grenoble.cnrs.fr

Perovskite-like oxides of Sr–Bi–TM–O systems (with TM = transition metal) have been extensively studied but surprisingly no structures have been published in the Sr–Bi–Ni–O system. Samples with nominal composition $\text{Sr}_3\text{Bi}_{2-x}\text{Ni}_x\text{O}_{6-\delta}$ were prepared from nitride precursors and calcined in air or oxygen current at 900 °C during

10–15 hours, followed by 20–30 hours at 1000–1200 °C. In the present transmission electron microscopy (TEM) study precession electron diffraction was carried out on a Philips CM300ST equipped with the spinning star precession unit. Chemical analysis was achieved by EDS in a Tecnai F20ST. TEM showed the existence of at least 3 different phases: a tetragonal phase ($a = 5.36 \text{ \AA}$, $c = 17.5 \text{ \AA}$), a closely related orthorhombic phase ($a_o \approx a_t / \sqrt{2}$, $b_o \approx a_t * \sqrt{2}$, $c_o \approx c_t$) and a minority cubic phase ($a = 33.7 \text{ \AA}$, 8.2% Ni, 64.1% Sr, 27.7% Bi) which represents not more than a few percent of the sample. In the case of a minority phase with a large unit cell X-ray powder diffraction is useless for structure determination. We therefore conducted an electron crystallography study on the cubic phase.

Due to the very large unit cell of the cubic phase the precession angle is limited by Laue zone overlap and was chosen as 0.8° or 1.3° depending on the zone axis. Systematic extinction and the symmetry of the higher order Laue zones indicated $Im\bar{3}m$ as the most probable space group. 6 zone axes yielded 1692 independent reflections. Using different input parameters for SIR2008 (starting composition, maximal resolution, applying or not a Lorentz correction) yielded the same cation positions with slightly different chemical order. The cations are ordered in layers alternating pure Sr layers and layers formed by Bi, Sr and Ni ions. In the mixed layers the cations are equally spaced forming a square lattice. In the Sr layers the distances between Sr rows alternate between 3.95 Å and 4.5 Å creating rectangles, small and large squares. The figure shows a Sr and a mixed layer.

Not all of the oxygen atoms were directly found but the ones present in the structure solutions clearly showed that the oxygen are in the center of the cation squares except for the 'large' squares in the Sr layers where the oxygen are on the square edges. The resulting composition is $\text{Sr}_{672}\text{Bi}_{272}\text{Ni}_{80}\text{O}_{1200}$ in agreement with the EDS measurements. To the best of our knowledge, this is the largest structure ever solved by precession electron diffraction.



Keywords: precession electron diffraction, structure solution, electron crystallography

MS79.P06

Acta Cryst. (2011) A67, C694–C695

Fourier images in coherent convergent beam electron diffraction and atomic resolution scanning transmission electron microscopy

Changlin Zheng,^a Joanne Etheridge,^{a,b} ^aMonash Centre for Electron Microscopy, Monash University, Victoria 3800 (Australia). ^bDepartment of Materials Engineering, Monash University, Victoria 3800 (Australia). E-mail: changlin.zheng@monash.edu

Fourier images (the Talbot effect) are a special self-imaging phenomenon arising from the coherent illumination of a periodic object. The formation mechanism has been carefully analyzed by J. M. Cowley and A. F. Moodie with diffraction theory in the 1950s [1].

Here we report the experimental observation of Fourier images in coherent convergent beam electron diffraction (CBED) patterns taken using high energy incident electrons. We use a transmission electron